



Variable Viscosity Impact on Peristaltic Transport of Hybrid Nanomaterial in Tapered Channel

Alaa Waleed Salih^{1*}   and Ahmed M. Abdulhadi²  

^{1,2}Department of Mathematics, College of Science, University of Baghdad, Baghdad, Iraq.

*Corresponding Author.

Received: 15 January 2024

Accepted: 6 May 2024

Published: 20 July 2025

doi.org/10.30526/38.3.3897

Abstract

This present study focuses on the analysis of peristaltic transport involving hybrid nanomaterial fluid through a tapered channel. Peristalsis of hybrid nanomaterial with variable viscosity is studied here. Thermal heat and velocity with no-slip conditions are considered in the investigation. In order to simplify governing equations small Reynolds number and large wavelength assumptions are used, the exact solution for formulation of stream function, axial velocity and temperature are determined based on the perturbation technique. In the present study, water is used as a head liquid while nanoparticle contains polystyrene and graphene oxide. Additionally, main purpose is to explain impacts of various physical parameter and porosity parameter. Here, we are concerned with studying the influences of heat transfer and porous medium on MHD of hybrid nanomaterial which translates through a two dimensional asymmetric, tapered channel. Finally, the plot of expressions of velocity curve, temperature distribution and streamlines with trapping phenomena are obtained via Mathematica 11 software.

Keywords : Hybrid nanomaterial, Variable viscosity, Peristaltic transport, Tapered channel.

1.Introduction

Peristaltic transport of fluid is an essential tool of almost biological and industrial procedures. On the other hand various studies associated with this phenomenon, because of its excellent importance as well as the distinctive aspects. We can be observed peristalsis significant in the flow processes; for detail, the transport of kidneys urine, chyme motion with tract of gastrointestinal and activity of motion of the food through digestive tract. After the basis work when appeared wide application of peristalsis flow and pulled researchers attention as shown in (1). In (2) displayed the peristaltic transport of a Newtonian fluid with variable viscosity in an asymmetric channel. Authors in (3) analyzed the effect of variable viscosity on hydro magnetic boundary layer.

The flow of peristaltic has been taken active interest through magnetic fields and considered via students and researchers when observe the thickening of viscosity of liquid depend on magnetic field (4-6). Furthermore, (7) studied peristaltic transport with heat and mass transfer of MHD through a compliant porous channel. (8) examined the impact of induced



magnetic on mixed heat transfer through peristalsis movement .Via (9-13) discuss that the idea , under effects of heat source the peristaltic flow with nanofluid in an inclined channel with two walls for non-Newtonian fluid. (14) Sheriff et al. dealt with different forms of nanoparticles in a non-uniform channel . The mechanism of peristalsis has been proven to be very helpful in transportation of liquid. Authors in (15) considered the influences of heat source, and inclined magnetic field in the tapered asymmetric channel through a porous medium.

The phenomenon of peristaltic transport of hybrid nanomaterial through the activity of viscous looked at by (16) .

In Non-Newtonian fluids, which have variable viscosity of fluid, in which particle size is taken into account and studied via (17). Also, (18) had modeled the peristaltic flow of bingham plastic fluid with variable viscosity in an inclined tapered asymmetric channel. Recently, researchers have been seen at a magnetic field and influence of mass and heat transfer for the motion of peristaltic due to their wide range between industrial and engineering . For more elements , We have theoretically analyzed the problem of peristaltic transport of a viscoelastic fluid in the tapered micro channel with variable viscosity. Almost of above cited studies deal with constant viscosity but extremely attractive to obtain impact of changeable viscosity .In addition, (19-22) the authors discussed influence of variable viscosity on peristaltic motion through various channel. (23) examined the impact of couple stress on peristaltic transport of a Powell-Eyring fluid in an inclined asymmetric channel.

Hybrid nanomaterials are considered as unique chemical combination of organic and/or inorganic materials. Various researchers groups are continuously presenting new studies a round the world about hybrid nanomaterial with application of it . Almost studies have been interested in role of this kind of nanomaterial with peristalsis flow investigated via (24-27) . the Influence of a rotation and heat transform in an inclined asymmetric channel with effect of different parameters studied by (29). (30) and (31) considered impacts of Magnetic Force, heat transfer and non-uniform channel for Peristaltic Transport of Non-Newtonian, Fluid .Influence of some fluid mechanic parameters caused from heat transport have discussed by (32) .On the other hand study of entropy generation can be very useful in different studies of nanomaterial flow of peristaltic disclosed by (33, 43). Many researchers analysis the combined influences of hybrid nanoliquid in the efficiency of engineering systems for more details see (34,35,38,39,40). In (36) , authors explain utilization of modified Darcy's law in peristalsis with a compliant channel through applications to thermal science . (37) considered inclined magnetic field, heat transfer and Porous Medium of asymmetric Channel on hyperbolic tangent peristaltic flow. The study of MHD features in peristaltic motion having impactful role in fluid flow . In (41), analysis effect of MHD and porous media, on peristaltic transport for nanofluids in an asymmetric channel for different types of walls. Analysis for variable viscous couple stress fluid flow through a channel with non-uniform wall temperature examined via (42). Here, we share in this investigations the reader through (44-47) to describe effect of analysis for varying of viscous through peristaltic tube or channel . Furthermore,, various studies (48-52) accounted tapered, channel duo to peristaltic transport with fluid flow .

The aim focus in this paper displayed analytical expessions for base fluid (water) and nanoparticles flow behavior in tapered channel where porous medium existing . Through a quick look at the changes that have been represented by graphs . This research is designed to determine and explain the effects of magnetic field , Hart mann number , porosity parameter and various boundaries on temperature, axial velocity, pressure gradient profiles respectively, The exact solution is calculated by Mathematica (11) software .

2. Materials and Methods

2.1. A mathematical formulation for tapered asymmetric flow

Establish the MHD fluid transport through tapered asymmetric channel with variable viscosity, two dimensions with porous medium and width of (d_1+d_2) . peristaltic motion considered by sinusoidal waves with constant speed (c) along the walls of channel .

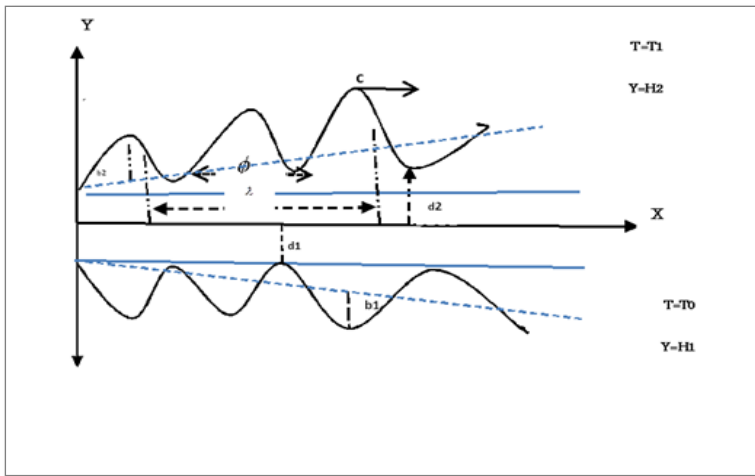


Figure 1. Geometric diagram of the tapered asymmetric channel.

The channel walls equations are presented as

$$H_1 = d_1 + \bar{k} \bar{X} + b_1 \sin \left[\frac{2\pi}{\lambda} (\bar{X} - c\bar{t}) \right], \quad \text{Lower wall} \quad (1)$$

$$H_2 = -d_2 - \bar{k} \bar{X} - b_2 \sin \left[\frac{2\pi}{\lambda} (\bar{X} - c\bar{t}) + \varphi \right] \quad \text{Upper wall} \quad (2)$$

Where (b_1) and (b_2) display wave amplitudes of the lower and upper walls, respectively. (c) represent the velocity of peristaltic wave, \bar{t} is the time, λ is the wave length, the phase difference (φ) at range $0 \leq \varphi \leq \pi$, and $(\bar{k} \ll 1)$ is a non- uniform parameter. Cartesian coordinates are represented by (\bar{X}, \bar{Y}) , where the transverse axis is \bar{Y} which is perpendicular to \bar{X} , and the axis of channel is \bar{X} . d_1 , and d_2 denoted to the fixed top of the higher and lesser walls of from center line respectively. Moreover, b_1, b_2, d_1, d_2 and φ satisfy the following relation at inlet of divergent channel:

$$b_1^2 + b_2^2 + 2b_1b_2 \cos(\varphi) \leq (d_1 + d_2)^2 \quad (3)$$

2.2. Governing equations of Problem

The mastering governing equations of hybrid nanomaterial fluid example with varying viscosity from one side to the other in tapered channel through laboratory frame are.

The Continuity Equations:

$$\frac{\partial \bar{u}}{\partial x} + \frac{\partial \bar{v}}{\partial y} = 0 \quad (4)$$

The Momentum Equations:

$$\rho_{hnf} \left[\frac{\partial \bar{u}}{\partial t} + u \frac{\partial \bar{u}}{\partial x} + v \frac{\partial \bar{u}}{\partial y} \right] = -\frac{\partial \bar{p}}{\partial x} + 2 \frac{\partial}{\partial x} \left[\bar{\mu}(T) \frac{\partial \bar{u}}{\partial x} \right] + \frac{\partial}{\partial y} \left[\bar{\mu}(T) \left[\frac{\partial \bar{u}}{\partial x} + \frac{\partial \bar{u}}{\partial y} \right] \right] - \sigma_{hnf} B_0^2 \bar{u} - \frac{\bar{\mu}(T)}{k} \bar{u} \quad (5)$$

$$\rho_{hnf} \left[\frac{\partial \bar{v}}{\partial t} + u \frac{\partial \bar{v}}{\partial x} + v \frac{\partial \bar{v}}{\partial y} \right] = -\frac{\partial \bar{p}}{\partial y} + 2 \frac{\partial}{\partial x} \left[\bar{\mu}(T) \frac{\partial \bar{v}}{\partial x} \right] + \frac{\partial}{\partial y} \left[\bar{\mu}(T) \left[\frac{\partial \bar{v}}{\partial x} + \frac{\partial \bar{v}}{\partial y} \right] \right] \quad (6)$$

The Energy Equation

$$\left[\rho_p \left[\frac{\partial \bar{T}}{\partial t} + u \frac{\partial \bar{T}}{\partial x} + v \frac{\partial \bar{T}}{\partial y} \right] \right] = k_{hmf} \left[\frac{\partial^2 \bar{T}}{\partial y^2} + \frac{\partial^2 \bar{T}}{\partial x^2} \right] + \bar{\mu}(\bar{T}) \left[2 \left\langle \left\langle \frac{\partial \bar{u}}{\partial x} \right\rangle \right\rangle + \left\langle \left\langle \frac{\partial \bar{v}}{\partial y} \right\rangle \right\rangle \right] + \left\langle \left\langle \frac{\partial \bar{u}}{\partial x} + \frac{\partial \bar{v}}{\partial y} \right\rangle \right\rangle + \sigma_{hmf} B_o^2 \bar{u}^2 + \bar{\phi}_o, \tag{7}$$

Where \bar{u} represents the axial velocity along \bar{x} - directions, \bar{v} represents the transverse velocity along \bar{y} - directions, and the temperature is \bar{T} .

ρ_{hmf} , σ_{hmf} , $\langle \rho_p \rangle_{hmf}$, B_o , $\bar{\phi}_o$ and k_{hmf} denoted to the effective density, electrical conductivity, heat capacitance, magnetic strength, heat absorption coefficient and thermal conductivity for hybrid nanomaterials ,respectively.

However, the relationship between the two frames is displayed for stable flow by the

following form and it can be treated as steady flow in a coordinate system (\bar{x}, \bar{y}) , where we switch from laboratory frame to wave frame.

$$\bar{x} = \bar{X} - c\bar{t}, \bar{u} = \bar{U} - c, \bar{p} = \bar{P}, \bar{y} = \bar{Y}, \bar{v} = \bar{V} \tag{8}$$

2.3.Solution of the problem

Let us introduce the next dimensionless quantities and variables as follows to simplify the governing equations:

$$\left. \begin{aligned} x = \frac{\bar{x}}{\lambda}, y = \frac{\bar{y}}{a}, u = \frac{\bar{u}}{c}, v = \frac{\bar{v}}{c\delta}, t = \frac{c\bar{t}}{\lambda}, \delta = \frac{a}{\lambda}, p = \frac{a^2 \bar{p}}{c\lambda M_f} \\ \mathcal{G} = \frac{\{\bar{T} - \bar{T}_o\}}{\bar{T}_o}, h_1 = \frac{H_1}{d_1}, h_2 = \frac{H_2}{d_1}, a = \frac{a_1}{d_1}, d = \frac{d_2}{d_1}, b = \frac{a_2}{d_1}, k = \frac{\bar{k}\lambda}{d_1} \\ M^2 = \frac{\sigma_f B_o^2 a^2}{\dots}, \beta = \frac{\bar{\phi}_o a^2}{\tau \dots}, \mu(\mathcal{G}) = \frac{\bar{\mu}(T)}{\dots}, D = \frac{a^2}{\dots}, R_e = \frac{\rho_f c a}{\dots} \end{aligned} \right\} \tag{9}$$

Here $\{x, y, u, v, \delta, a, b, t, p, \mathcal{G}, k, \beta, D, R_e\}$ are designate components of the dimensionless coordinates, dimensionless axial velocity, dimensionless transverse velocity, number of wave, amplitudes of lower wall, amplitudes of upper wall, dimensionless time, dimensionless pressure, temperature, non-uniform parameter, heat sink/source parameter, porosity parameter, the Reynolds number. μ_0 is refer to constant viscosity, $\Delta T = T_1 - T_0$ is the temperature difference, where T_0 and T_1 are refer to the temperature in the lower and upper wall, respectively.

As $U(x, y, t)$ and $V(x, y, t)$ refer to the components of velocity along x –direction and y –direction respectively.

Now, By applying the dimensionless variables in Equation (9), with flow being steady,

Equations (4-7) become as follow .

$$\frac{\partial u}{\partial x} + \frac{\partial v}{\partial y} = 0, \tag{10}$$

$$R_e \delta \left[\frac{\partial u}{\partial t} + u \frac{\partial u}{\partial x} + v \frac{\partial u}{\partial y} \right] = - \frac{\partial p}{\partial x} + \frac{\partial}{\partial y} \left[\mu(\mathcal{G}) \frac{\partial u}{\partial y} \right] - \frac{\sigma_f B_o^2 a^2}{\mu_o} u - \mu(\mathcal{G}) \frac{a^2}{k_o} u, \tag{11}$$

$$R_e \delta^3 \left[\frac{\partial v}{\partial t} + u \frac{\partial v}{\partial x} + v \frac{\partial v}{\partial y} \right] = -\frac{\partial p}{\partial y} + 2\delta^3 \frac{\partial}{\partial x} \left[\mu(\vartheta) \frac{\partial v}{\partial y} \right] + \frac{\partial}{\partial y} \left[\mu(\vartheta) \left[\delta^3 \frac{\partial v}{\partial x} + \delta^2 \frac{\partial v}{\partial y} \right] \right], \quad (12)$$

Implementing via long-wavelength ($\delta \ll 1$) and approximating of small Reynolds number which are simplest way . In addition, by using the relation ship between stream function ψ and velocity components that is defined down in Equation (13).

$$u = \frac{\partial \psi}{\partial y} \quad v = -\delta \frac{\partial \psi}{\partial x} \quad (13)$$

Then we obtain Equation (11) and Equation (12) become:

$$\frac{\partial \psi}{\partial x \partial y} - \frac{\partial \psi}{\partial y \partial x} = 0, \quad (14)$$

$$\frac{\partial p}{\partial x} = \frac{\partial}{\partial y} \left[\mu(\vartheta) \frac{\partial u}{\partial y} \right] - [M^2 + D\mu(\vartheta)]u, \quad (15)$$

$$\frac{\partial p}{\partial x} = \frac{\partial}{\partial y} \left[\mu(\vartheta) \frac{\partial^2 \psi}{\partial y^2} \right] - M^2 \left[\frac{\partial \psi}{\partial y} \right] - \mu(\vartheta) D \left[\frac{\partial \psi}{\partial y} \right], \quad (16)$$

$$\frac{\partial p}{\partial y} = 0, \quad (17)$$

$$\frac{\partial^2 \vartheta}{\partial y^2} + \beta = 0, \quad (18)$$

The system that appear above will be solved analytically to get dimensionally format for velocity (u), and temperature denoted via ϑ of nonlinear peristalsis transport with temperature disposed viscosity parameters .

In the implied paper, the exponential dependence of viscosity on temperature is named (20, 28) as the next expression :

$$\mu(\vartheta) = e^{-\varepsilon \vartheta}, \quad (19)$$

Where (ε) is viscosity parameter which is a constant for ($\varepsilon \ll 1$) .by using Taylor expansion and neglecting square and higher power of ε , then we obtain

$$\mu(\vartheta) = 1 - \varepsilon \vartheta \quad (20)$$

$$\frac{\partial p}{\partial x} = \frac{\partial}{\partial y} \left[(1 - \varepsilon \vartheta) \frac{\partial^2 \psi}{\partial y^2} \right] - M^2 \left[\frac{\partial \psi}{\partial y} \right] - D(1 - \varepsilon \vartheta) \left[\frac{\partial \psi}{\partial y} \right], \quad (21)$$

$$0 = (1 - \varepsilon \vartheta) \frac{\partial^4 \psi}{\partial y^4} - 2\varepsilon \frac{\partial \vartheta}{\partial y} \frac{\partial^3 \psi}{\partial y^3} - \varepsilon \frac{\partial^2 \vartheta}{\partial y^2} \frac{\partial^2 \psi}{\partial y^2} - M^2 \frac{\partial^2 \psi}{\partial y^2} - D(1 - \varepsilon \vartheta) \frac{\partial^2 \psi}{\partial y^2} + D\varepsilon \frac{\partial \vartheta}{\partial y} \frac{\partial \psi}{\partial y} \quad (22)$$

The suitable boundary conditions in non-dimensional wave frame are as follows:

Part

$$\begin{aligned} \psi = 0, \quad \frac{\partial^2 \psi}{\partial y^2} = 0, \quad \frac{\partial \vartheta}{\partial y} = 0 \quad \text{at } y = h_1 \\ \psi = F, \quad \frac{\partial \psi}{\partial y} = -1, \quad \vartheta + \gamma \frac{\partial \vartheta}{\partial y} = 0, \quad \text{at } y = h_2 \end{aligned} \quad (23)$$

Where above (γ) present thermal slip parameter and F is the non- dimensional mean flow rate in the wave frame.

The non-dimensional forms of the lower and upper walls are:

$$h_1 = 1 + k(x + t) + a \sin(2\pi x) \tag{24}$$

$$h_2 = -d - k(x + t) - b \sin(2\pi x + \varphi) \tag{25}$$

2.4. Perturbation solutions and Analytical

2.4.1. Zero-order system:

Identified zero –order system by the following..

$$0 = \frac{\partial^4 \psi_0}{\partial y^4} - M^2 \frac{\partial^2 \psi_0}{\partial y^2} - D \frac{\partial^2 \psi_0}{\partial y^2} \tag{26}$$

The equivalent boundary conditions have been :

$$\psi_0 = 0 \quad , \quad \frac{\partial^2 \psi_0}{\partial y^2} = 0 \quad , \quad \text{at } y = h_1 \quad , \quad \& \quad \psi_0 = F_0 \quad , \quad \frac{\partial \psi_0}{\partial y} = -1 \quad , \quad \text{at } y = h_2. \tag{27}$$

The solution of the transport Eq.(26) subjected to the conditions in Eq. (27) has the next form

$$\psi_0 = c_5 + a_2 c_4 e^{-a_3 y} + a_2 c_3 e^{a_3 y} + c_6 y, \tag{28}$$

Where

$$\left. \begin{aligned} c_3 &= - \frac{e^{a_3 h_2} (F_0 - h_1 + h_2)}{a_2 (e^{2a_3 h_1} - e^{2a_3 h_2} - a_3 e^{2a_3 h_1} h_1 - a_3 e^{2a_3 h_1} h_2 + a_3 e^{2a_3 h_1} h_2 + a_3 e^{2a_3 h_2} h_2)}, \\ c_4 &= \frac{e^{2a_3 h_2 + a_3 h_2} (-F_0 + h_1 - h_2)}{a_2 (-e^{2a_3 h_1} + e^{2a_3 h_2} + a_3 e^{2a_3 h_1} h_1 + a_3 e^{2a_3 h_2} h_1 - a_3 e^{2a_3 h_1} h_2 - a_3 e^{2a_3 h_2} h_2)}, \\ c_5 &= - \frac{h_1 (-e^{2a_3 h_1} + e^{2a_3 h_2} + a_3 e^{2a_3 h_1} F_0 + a_3 e^{2a_3 h_2} F_0)}{(e^{2a_3 h_1} + e^{2a_3 h_2} + a_3 e^{2a_3 h_1} h_1 + a_3 e^{2a_3 h_2} h_1 - a_3 e^{2a_3 h_1} h_2 - a_3 e^{2a_3 h_2} h_2)}, \\ c_6 &= \frac{(-e^{2a_3 h_1} + e^{2a_3 h_2} + a_3 e^{2a_3 h_1} F_0 + a_3 e^{2a_3 h_2} F_0)}{(-e^{2a_3 h_1} + e^{2a_3 h_2} + a_3 e^{2a_3 h_1} h_1 + a_3 e^{2a_3 h_2} h_1 - a_3 e^{2a_3 h_1} h_2 - a_3 e^{2a_3 h_2} h_2)}, \end{aligned} \right\} \tag{29}$$

The first-order system is got as :

$$0 = \frac{\partial^4 \psi_1}{\partial y^4} - g \frac{\partial^4 \psi_0}{\partial y^4} - 2 \frac{\partial g}{\partial y} \frac{\partial^3 \psi_0}{\partial y^3} - \frac{\partial^2 g}{\partial y^2} \frac{\partial^2 \psi_0}{\partial y^2} - M^2 \frac{\partial^2 \psi_1}{\partial y^2} - D g \frac{\partial^2 \psi_0}{\partial y^2} - D \frac{\partial^2 \psi_1}{\partial y^2} + D \frac{\partial g}{\partial y} \frac{\partial \psi_0}{\partial y}, \tag{30}$$

With equivalent boundary conditions such as:

$$\psi_1 = 0 \quad , \quad \frac{\partial^2 \psi_1}{\partial y^2} = 0 \quad , \quad \text{at } y = h_1 \quad , \quad \& \quad \psi_1 = F_1 \quad , \quad \frac{\partial \psi_1}{\partial y} = 0 \quad , \quad \text{at } y = h_2 \tag{31}$$

The solution for first-order problem Eq.(30) subjected to conditions in Eq.(31) has been consistent as:

$$\begin{aligned} (32) \quad \psi_1 &= s_3 + s_2 \frac{e^{-\sqrt{a_1} y}}{a_1 - a_3^2} - a_3^2 s_2 \frac{e^{-\sqrt{a_1} y}}{a_1 (a_1 - a_3^2)} + s_1 \frac{e^{\sqrt{a_1} y}}{a_1 - a_3^2} - a_3^2 s_1 \frac{e^{\sqrt{a_1} y}}{a_1 (a_1 - a_3^2)} \\ &- a_2 a_4 c_4 \frac{e^{a_3 y}}{a_1 - a_3^2} + s_4 y - a_2 a_3^2 c_4 \frac{e^{-a_3 y}}{a_1 - a_3^2} g - a_2 a_3^2 c_3 \frac{e^{a_3 y}}{a_1 - a_3^2} g + 2 a_2 a_3 c_4 \frac{e^{-a_3 y}}{a_1 - a_3^2} g_1 \\ &- 2 a_2 a_3 c_3 \frac{e^{a_3 y}}{a_1 - a_3^2} g_1 - a_2 c_4 \frac{e^{-a_3 y}}{a_3 (a_1 - a_3^2) D} g_1 + a_2 c_3 \frac{e^{a_3 y}}{a_3 (a_1 - a_3^2) D} g_1 + c_6 \frac{y^2 g_1}{2(a_1 - a_3^2) D} \\ &- a_3^2 c_6 \frac{y^2 g_1}{2 a_1 (a_1 - a_3^2) D} \end{aligned} \tag{32}$$

2.4.2. Solution of temperature:

the solution of temperature Eq.(18) is obtained from system subject to the boundary conditions of non- dimensional temperature \mathcal{G} in the wave frame as follows:

$$\left. \begin{aligned} \text{At } y = h_1, \quad \frac{\partial \mathcal{G}}{\partial y} = 0, \\ \text{At } y = h_2, \quad \mathcal{G} + \gamma \frac{\partial \mathcal{G}}{\partial y} = 0 . \end{aligned} \right\} \quad (33)$$

The exact solution of temperature, that satisfies the boundary conditions (33), can be obtained as:

$$\mathcal{G} = \frac{-y^2}{2} \beta + c_1 + \gamma c_2 \quad (34)$$

Where,

$$c_1 = \left(-h_1 h_2 + \frac{1}{2} h_2^2 - h_1 \gamma + h_2 \gamma \right) \beta, \quad (35)$$

$$c_2 = h_1 \beta,$$

In addition, the momentum equation (22) is non-linear. Then, the perturbation method is used for a small fluid parameter (ε) and to identify approximate series solutions of Eq.(22).The stream function is expanded in powers of (ε) as follows:

$$\psi = \psi_0 + \varepsilon \psi_1 + \varepsilon^2 \psi_2 + \dots \quad (36)$$

By substituting Eq.(28) & (32) into Eq. (36)and the coefficients are compare of the same power of up to the first order, we obtain the next equation ..

$$\begin{aligned} \psi = c_5 + a_2 c_4 e^{-a_3 y} + a_2 c_3 e^{a_3 y} + c_6 y + \varepsilon [s_3 + s_2 \frac{e^{-\sqrt{a_1} y}}{a_1 - a_3^2} - a_3^2 s_2 \frac{e^{-\sqrt{a_1} y}}{a_1(a_1 - a_3^2)} + s_1 \frac{e^{\sqrt{a_1} y}}{a_1 - a_3^2} \\ - a_3^2 s_1 \frac{e^{\sqrt{a_1} y}}{a_1(a_1 - a_3^2)} - a_2 a_4 c_4 \frac{e^{a_3 y}}{a_1 - a_3^2} + s_4 y - a_2 a_3^2 c_4 \frac{e^{-a_3 y}}{a_1 - a_3^2} \mathcal{G} - a_2 a_3^2 c_3 \frac{e^{a_3 y}}{a_1 - a_3^2} \mathcal{G} \\ + 2a_2 a_3 c_4 \frac{e^{-a_3 y}}{a_1 - a_3^2} \mathcal{G}_1 - 2a_2 a_3 c_3 \frac{e^{a_3 y}}{a_1 - a_3^2} \mathcal{G}_1 - a_2 c_4 \frac{e^{-a_3 y}}{a_3(a_1 - a_3^2)} D \mathcal{G}_1 + a_2 c_3 \frac{e^{a_3 y}}{a_3(a_1 - a_3^2)} D \mathcal{G}_1 \\ + c_6 \frac{y^2 \mathcal{G}_1}{2(a_1 - a_3^2)} D - a_3^2 c_6 \frac{y^2 \mathcal{G}_1}{2a_1(a_1 - a_3^2)} D] \end{aligned} \quad (37)$$

The amounts of various coefficients $\{c_3, c_4, c_5, c_6, s_1, s_2, s_3, s_4\}$ are long non-constant and their values can be determined with boundary conditions(no-slip) in Eq. (26)&(30)via using Mathematica 11 software.

3. Results and Discussions

In this section of paper, we discussed the graphical illustration for the variable viscosity(u) of hybrid nanomaterials, temperature (ϑ), the variation of pressure gradient ($\frac{dp}{dx}$), and streamlines contours . The plotted outcomes of almost various physical variables that produced by Mathematica software version -11.

3.1. Velocity Profile.

The graphs of velocity curve show that the behavior of distribution is parabolic in nature. The curve was drawn for fixed values of $\{x = 0.7, t = 0.3\}$, **Figure (2)** shows the impact of non-uniform

parameter (k) on velocity distribution .As we seen in **Figure (2)** and **Figure 3**. the increasing in the value of k & M lead to increase of velocity curve ,while as shown in **Figure (3)** and **Figure (5)** the decreasing of the velocity distribution due to increase the rang of β & γ .

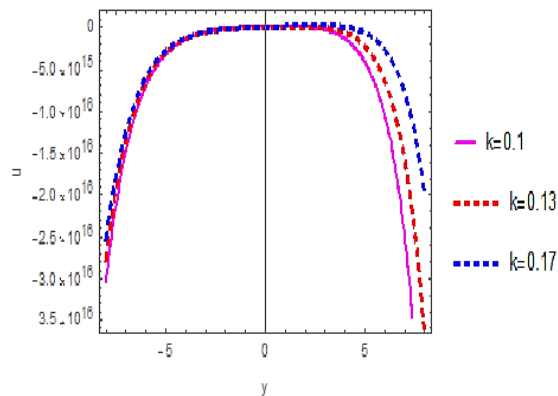


Figure 2. Impact of k on velocity profile (u) .

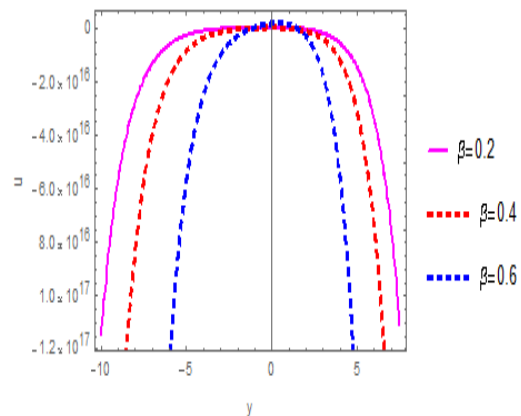


Figure 3. Impact of β on velocity profile (u) .

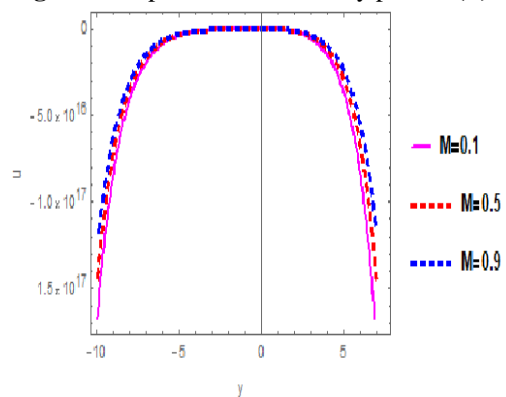


Figure 4. Impact of M on velocity profile (u) .

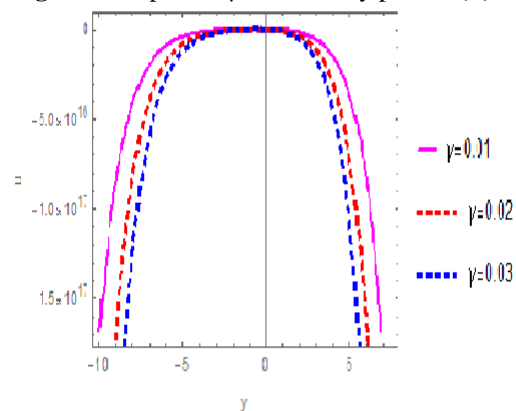


Figure 5. Impact of γ on velocity profile (u) .

3.2. Temperature Profile

The effect of various variables that explain in the temperature profile through **Figures (6-9)**. A parabolic behavior is determined via current temperature distribution against y -axis. As we observe in **Figures (6)** and **(7)**, the decreasing in temperature ϑ distribution return to increase of different values of a & b . Additionally, this profile as examined by **Figures (8)** and **(9)** the rise in distribution of (ϑ) due to increasing in (γ) and (ϕ) .

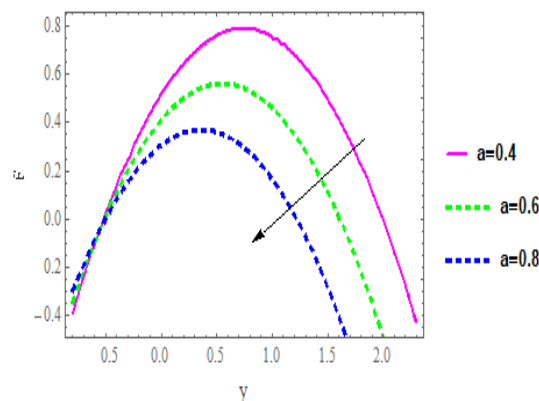


Figure 6. Impact of (a) on profile of temperature denoted by (ϑ) .

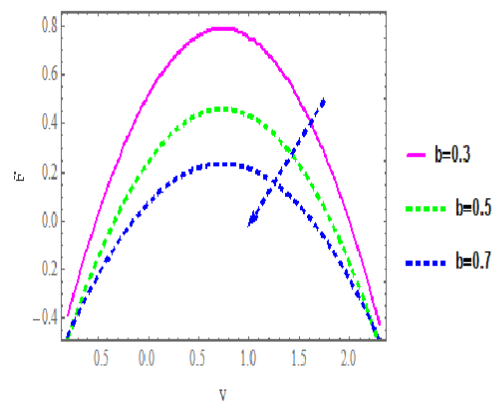


Figure 7. Impact of (b) on profile of temperature denoted by (ϑ) .

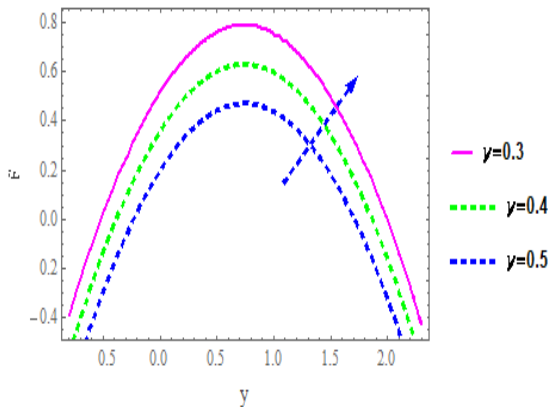


Figure 8. Impact of (γ) on profile of temperature denoted by (9) .

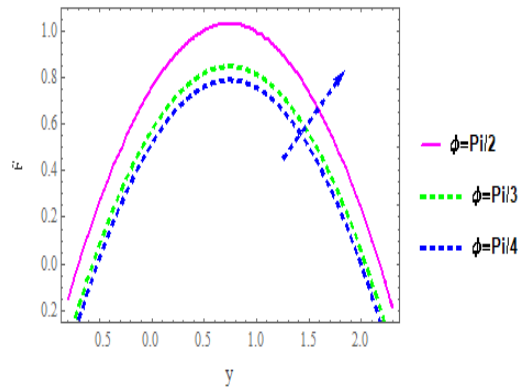


Figure 9. Impact of (ϕ) profile of temperature denoted by (9) .

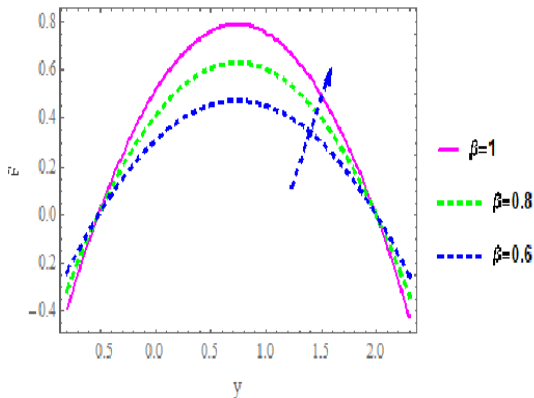


Figure 10. Impact of β on profile of temperature denoted by (9) .

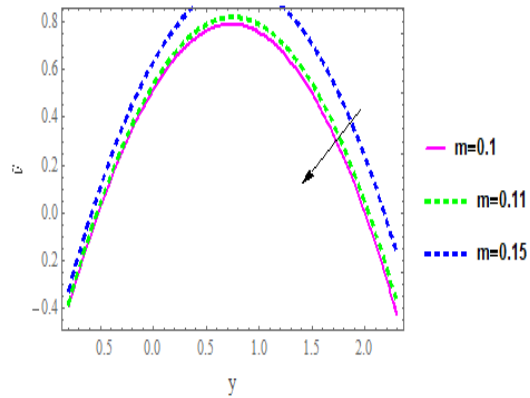


Figure 11. Impact of m on profile of temperature denoted by (9) .

3.3. Pressure Gradient Profile

Figures (12-15) show the variation of the pressure gradient profile with respect to various physical parameters . Almost Figures, these are illustrated that the profile of pressure gradient distribution that increases with the increase in values of parameter . we noticed that oscillatory behavior for dp/dx . It can be observed from **Figures (12)** and **(13)** increasing for different values of porosity parameter (D) and values of non-uniform parameter (k) respectively, led to increased in pressure gradient as shown in model. Also, In **Figures (14)** and **(15)** displayed that , the impact of variations in pressure gradient with respect to increases in different values of (φ) ,and Hartmann number (M) .

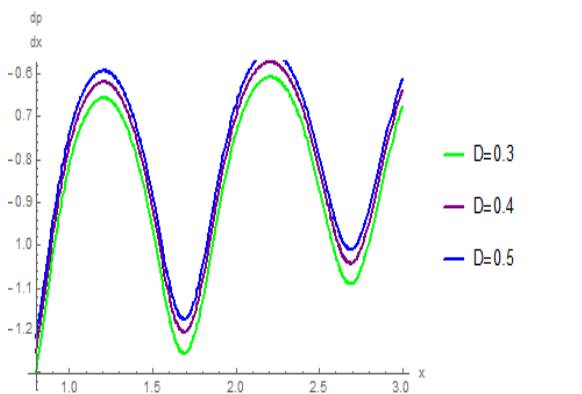


Figure 12. Impact of D on Pressure gradient profile $(\frac{dp}{dx})$.

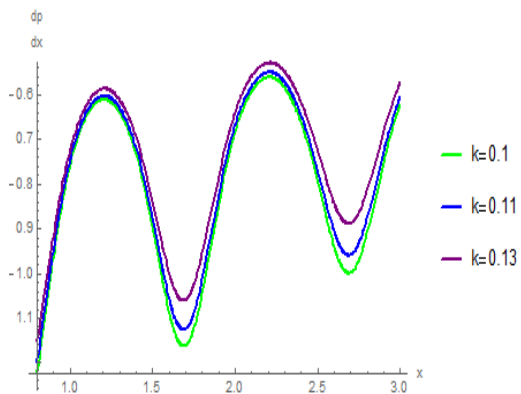


Figure 13. Impact of k on Pressure gradient profile $(\frac{dp}{dx})$.

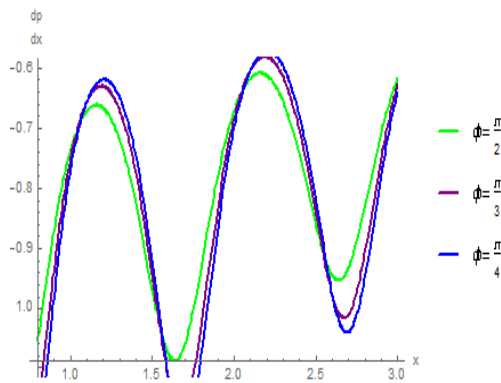


Figure 14. Impact of ϕ on Pressure gradient profile $\left(\frac{dp}{dx}\right)$.

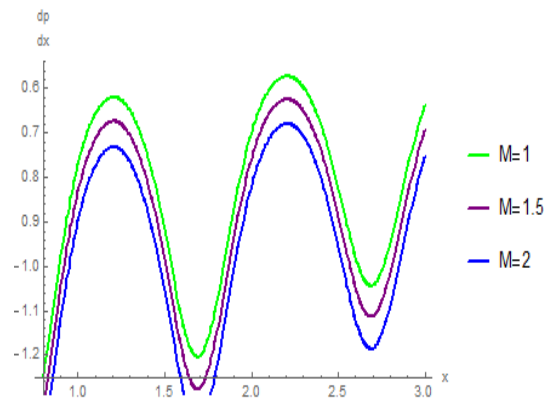


Figure 15. Impact of M on Pressure gradient profile $\left(\frac{dp}{dx}\right)$.

3.4. Trapping Phenomenon

In this subsection we will discuss and analyze the impact of some parameters on it . Formation of trapping via the disconnecting of streamlines , where the closed streamlines of the bolus are formed with respect to the peristaltic motion of the wall of the transport that apply on fluid flow within the channel .In order to explain effects of trapping phenomenon at different values of porosity parameter (D) , Hartmann number (M) , and viscosity parameter respectively . It can be observed from **Figure (16)** that when increases in value of M , the rises of trapped bolus. As **Figure (17)** illustrated the trapped bolus of tapered channel increases in size with the increase in porosity parameter.

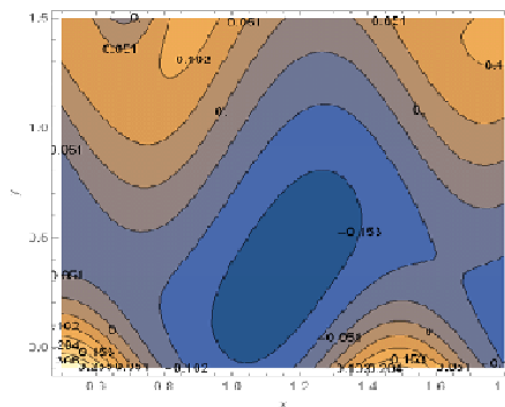
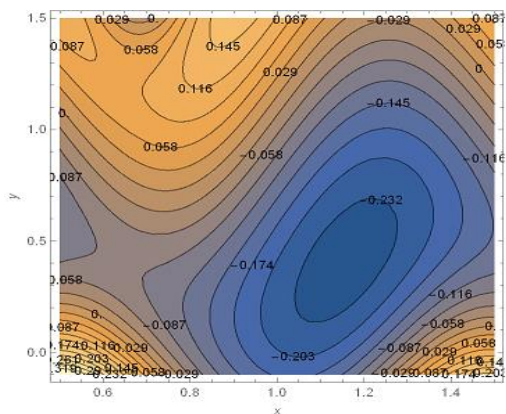


Figure 16. The impact of Hartmann (M) on streamlines

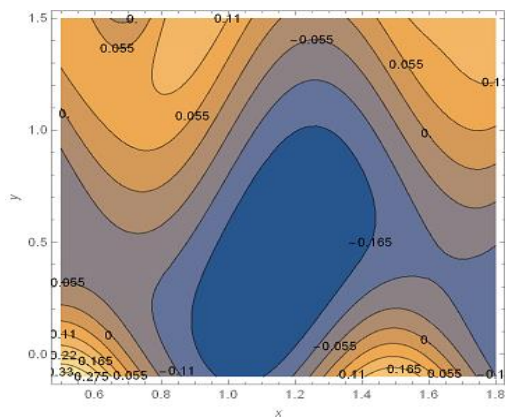
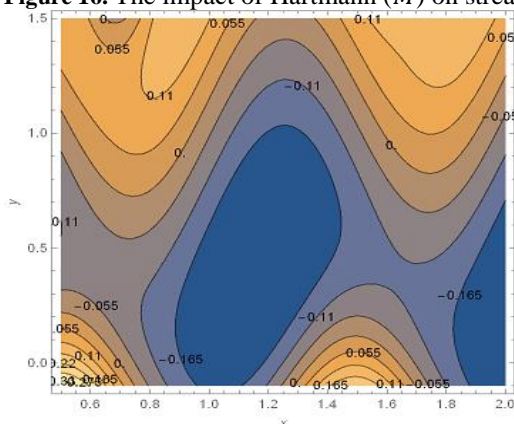


Figure 17. The impact of porosity parameter (D) on streamlines.

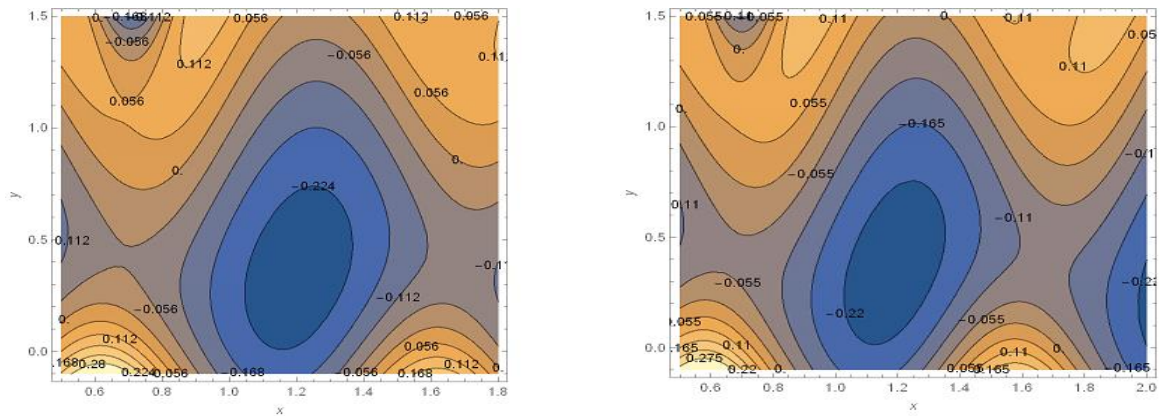


Figure 18. The impact of viscosity parameter (ε) on streamlines

4. Conclusion

In this section, we present the influences of variable viscosity and porous medium of hybrid nanomaterial fluid in tapered channel. The study is formulated by incorporating boundary condition, Coupled nonlinear equations are simplified by adopting large wavelength and small Reynolds number approach. Here, essential findings through numerical representation, due to the exhibited analysis the next outcomes are the main lines we obtained.

- It can be observed that, the velocity curve is parabolic path and increase near middle of channel , But at the walls part of the channel we note the distribution of velocity emanation due to increasing amount of parameters.
- Note that , The temperature(ϑ) versus y-axis as shown in above Figs. , Where profile of it diminishes upon decreasing almost parameters and increasing with others .
- For instance , Both of velocity and temperature profile respectively announced the same behavior toward various parameters .
- Pressure gradient diverges and increases with Hartmann number as well as the amount of (φ) on tapered channel .
- Generally, in the phenomenon of trapping that observes peristaltic motion of hybrid nanomaterial fluid under certain conditions , where the size of the trapped bolus increases as the values of (D) and (ε).

Acknowledgements

We would like to express our gratitude other referees for their valuable comments and suggestions that led to a truly significant improvement of the paper.

Conflict of Interest

The authors declare that they have no conflicts of interest.

Funding

This work is not supported by any the Foundation.

Ethical Clearance

Ethics of scientific research were carried out in accordance with international conditions .

References

1. Shapiro A.H., Jaffrin M.Y., Weinberg S.L. Peristaltic pumping with long wavelength at low Reynolds number. *J Fluid Mech* 1969;37(4):799–825. <https://doi.org/10.1017/S0022112069000899>
2. Hayat T., Ali N. Effect of variable viscosity on the peristaltic transport of a Newtonian fluid in an asymmetric channel. *Appl Math Model* 2008;32:761–774. <https://doi.org/10.1016/j.apm.2007.02.010>
3. Das U.J. Effects of variable viscosity on hydromagnetic boundary layer along a continuously moving vertical plate in the presence of radiation and chemical reaction. *J Electromagn Anal Appl* 2013;5(1):5–9. <https://doi.org/10.4236/jemaa.2013.51002>.
4. Prakash E., Siva P., Govindarajan A., Vidhya M. Influence of variable viscosity on peristaltic motion of a viscoelastic fluid in a tapered microfluidic vessel. *Int J Eng Technol* 2018;7(4.10):49–54. <https://doi.org/10.14419/ijet.v7i4.10.20705>
5. Kareem R.S., Abdulhadi A.M. Effect of MHD and porous media on nanofluid flow with heat transfer: numerical treatment. *J Adv Res Fluid Mech Therm Sci* 2019;63(2):317–328.
6. Hummady L.Z., Abbas I.T., Mohammed R.A. Inclined magnetic field of non-uniform and porous medium channel on couple stress peristaltic flow and application in medical treatment (knee arthritis). *J Southwest Jiaotong Univ* 2019;54(4). <https://doi.org/10.35741/issn.0258-2724.54.4.35>
7. Vaidya H., Rajashekhar C., Manjunatha G., Prasad K.V., Makinde O.D., Vajravelu K. Heat and mass transfer analysis of MHD peristaltic flow through a compliant porous channel with variable thermal conductivity. *Phys Scr* 2020. <https://doi.org/10.1088/1402-4896/ab681a>
8. Mohaisen H.N., Abdulhadi A.M. Effects of the rotation on the mixed convection heat transfer analysis for the peristaltic transport of viscoplastic fluid in asymmetric channel. *Iraqi J Sci* 2022;63(3):1240–1257. <https://doi.org/10.24996/ijs.2022.63.3.29>
9. Saleem A., Salman A., Fahad M.A. Physical aspects of peristaltic flow of hybrid nanofluid inside a curved tube having ciliated wall. *Results Phys* 2020;19:103431. <https://doi.org/10.1016/j.rinp.2020.103431>
10. Mohammed G.G., Salih A.W. Impacts of porous medium on unsteady helical flows of generalized Oldroyd-B fluid with two infinite coaxial circular cylinders. *Iraqi J Sci* 2021;62(5):1686–1694. <https://doi.org/10.24996/ijs.2021.62.5.31>.
11. Salih A.W., Habeeb S.B. Influence of rotation, variable viscosity and temperature on peristaltic transport in an asymmetric channel. *Turk J Math* 2021;12(6):1047–1059.
12. Ramesh K. Effects of slip and convective conditions on the peristaltic flow of couple stress fluid in an asymmetric channel through porous medium. *Comput Methods Programs Biomed* 2016;135:1–14. <https://doi.org/10.1016/j.cmpb.2016.07.001>
13. Awais M., Hayat T., Ali A., Irum S. Velocity, thermal and concentration slip effects on a magnetohydrodynamic nanofluid flow. *Alex Eng J* 2016;55:2107–2114. <https://doi.org/10.1016/j.aej.2016.06.027>
14. Nassief A.M., Abdulhadi A.M. Rotation and magnetic force effects on peristaltic transport of non-Newtonian fluid in a symmetric channel. *Ibn Al-Haitham J Pure Appl Sci* 2023;36(2):436–453. <https://doi.org/10.30526/36.2.3066>
15. Salih A.W., Habeeb S.B. Peristaltic flow with nanofluid under effects of heat source, and inclined magnetic field in the tapered asymmetric channel through a porous medium. *Iraqi J Sci* 2022;63(10):4445–4459. <https://doi.org/10.24996/ijs.2022.63.10.30>
16. Sheriff S., Ahmad S., Mir N.A. Irreversibility effects in peristaltic transport of hybrid nanomaterial in the presence of heat absorption. *Sci Rep* 2021;11:19697. <https://doi.org/10.1038/s41598-021-99229-7>.
17. Farooq S., Khan M.I., Waqas M., Hayat T., Alsaedi A. Transport of hybrid type nanomaterials in peristaltic activity of viscous fluid considering nonlinear radiation, entropy optimization and slip effects. *Comput Methods Programs Biomed* 2020;184:105086. <https://doi.org/10.1016/j.cmpb.2019.105086>

18. Hassen R.Y., Ali H.A. Hall and Joule's heating influences on peristaltic transport of Bingham plastic fluid with variable viscosity in an inclined tapered asymmetric channel. *Ibn Al-Haitham J Pure Appl Sci* 2021;34(1):68–84. <https://doi.org/10.30526/34.1.2554>
19. Akbar Y., Abbasi F.M. Impact of variable viscosity on peristaltic motion with entropy generation. *Int Commun Heat Mass Transfer* 2020;118:104826. <https://doi.org/10.1016/j.icheatmasstransfer.2020.104826>
20. Kareem R.S., Abdulhadi A.M. Impacts of heat and mass transfer on magnetohydrodynamic peristaltic flow having temperature-dependent properties in an inclined channel through porous media. *Iraqi J Sci* 2020;61(4):854–869. <https://doi.org/10.24996/ijs.2020.61.4.19>
21. Salman M.R., Hayat A.A. Approximate treatment for the MHD peristaltic transport of Jeffrey fluid in inclined tapered asymmetric channel with effects of heat transfer and porous medium. *Iraqi J Sci* 2020;61(12):3342–3354. <https://doi.org/10.24996/ijs.2020.61.12.22>
22. Salman M.R., Ahmed M.A. Influence of heat and mass transfer on inclined MHD peristaltic of pseudoplastic nanofluid through the porous medium with couple stress in an inclined asymmetric channel. *J Phys Conf Ser* 2018;1032(1):012043. <https://doi.org/10.1088/1742-6596/1032/1/012043>
23. Abdulhussein H., Abdulhadi A.M. Impact of couple stress and rotation on peristaltic transport of a Powell-Eyring fluid in an inclined asymmetric channel with Hall and Joule heating. *J Basic Sci* 2022;8(13):483–509.
24. Khan M.I., Alsaedi A., Niaz B.K., Hayat T. Modeling and computational analysis of hybrid class nanomaterials subject to entropy generation. *Comput Methods Programs Biomed* 2019;179:104973. <https://doi.org/10.1016/j.cmpb.2019.07.001>
25. Ramesh G.K., Shehzad S.A., Tlili I. Hybrid nanomaterial flow and heat transport in a stretchable convergent/divergent channel: a Darcy–Forchheimer model. *Appl Math Mech* 2020;41:699–710.
26. Nadeem A., Malik M.Y., Nadeem S. Transportation of magnetized micropolar hybrid nanomaterial fluid flow over a Riga surface. *Comput Methods Programs Biomed* 2020;185:105136. <https://doi.org/10.1016/j.cmpb.2019.105136>
27. Ahmed S.E., Rashed Z.Z. Magnetohydrodynamic dusty hybrid nanofluid peristaltic flow in curved channels. *Therm Sci* 2021;25(6) Part A:4241–4255. <https://doi.org/10.2298/TSCI191014144A>
28. Hosham H.A., Hafez N.M. Bifurcation phenomena in the peristaltic transport of non-Newtonian fluid with heat and mass transfer effects. *J Appl Math Comput* 2021;67(1–2):275–299. <https://doi.org/10.1007/s12190-020-01477-7>
29. Ibraheem R.G., Liqaa Z.H. Effect of different parameters on Powell–Eyring fluid peristaltic flow with the influence of a rotation and heat transform in an inclined asymmetric channel. *Baghdad Sci J* 2024;21(4):1318–1330. <https://doi.org/10.21123/bsj.2023.8360>
30. Abdulhussein H., Abdulhadi A.M. Impact of heat transfer and inclined MHD on a non-uniform inclined asymmetrical channel with couple stress fluid through a porous medium. *Iraqi J Sci* 2023;64(9):4580–4599. <https://doi.org/10.24996/ijs.2023.64.9.23>
31. Nassief A.M., Abdulhadi A.M. Influence of magnetic force for peristaltic transport of non-Newtonian fluid through porous medium in asymmetric channel. *Iraqi J Sci* 2023;64(7):3567–3586. <https://doi.org/10.24996/ijs.2023.64.7.35>
32. Zainab A.J., Hummady L.Z., Thawi M.H. Influence of some fluid mechanic parameters caused from heat transport with rotation on Walter's B fluid. *J Biomech Sci Eng* 2023;6(39). <https://doi.org/10.1007/s40430-017-0782-0>
33. Farooq S., Hayat T., Khan M.I., Alsaedi A. Entropy generation minimization in magneto peristalsis with variable properties. *Comput Methods Programs Biomed* 2020;186:105045. <https://doi.org/10.1016/j.cmpb.2019.105045>
34. Muhammad K., Hayat T., Alsaedi A. Numerical study for melting heat in dissipative flow of hybrid nanofluid over a variable thicked surface. *Int Commun Heat Mass Transfer* 2021;121:104805. <https://doi.org/10.1016/j.icheatmasstransfer.2020.104>
35. Aamir A., Mehak S., Hafiz J.A., Muhammad A., Kottakkaran S.N., Ahamed S.C. Entropy generation analysis of peristaltic flow of nanomaterial in a rotating medium through generalized

- compliant walls of micro-channel with radiation and heat flux effects. *Micromachines* 2022;13:375. <https://doi.org/10.3390/mi13030375>
36. Imran N., Javed M., Sohail M., Thili I. Utilization of modified Darcy's law in peristalsis with a compliant channel: applications to thermal science. *J Mater Res Technol* 2020;9(3):5619–5629. <https://doi.org/10.1016/j.jmrt.2020.03.087>
 37. Abdulla S.A., Hummady L.Z. Inclined magnetic field and heat transfer of asymmetric and porous medium channel on hyperbolic tangent peristaltic flow. *Int J Nonlinear Anal Appl* 2021;12(2):2359–2372. <http://dx.doi.org/10.22075/ijnaa.2021.5382>
 38. Salahuddin T., Muhammad H.U.K., Mair K., YuMing C. Peristaltically driven flow of hybrid nanofluid in a sinusoidal wavy channel with heat generation. *Phys Scr* 2020;96(2):025205. <https://doi.org/10.1088/1402-4896/abcd68>
 39. Wahab M.A., Erdem E.Y. Multi-step microfluidic reactor for the synthesis of hybrid nanoparticles. *J Micromech Microeng* 2020;30(8):085006. <https://doi.org/10.1088/1361-6439/ab8dd2>
 40. Muhammad K., Hayat T., Alsaedi A. Heat transfer analysis in slip flow of hybrid nanomaterial (ethylene glycol + Ag + CuO) via thermal radiation and Newtonian heating. *Waves Random Complex Media* 2021;1–21. <https://doi.org/10.1080/17455030.2021.1950947>
 41. Jawad Q.K., Abdulhadi A.M. Influence of MHD and porous media on peristaltic transport for nanofluids in an asymmetric channel for different types of walls. *Int J Nonlinear Anal Appl* 2023;14(1):819–832. <https://doi.org/10.22075/IJNAA.2022.6967>
 42. Falade J.A., Adesanya S.O., Ukaegbu J.C., Osinowo M.O. Entropy generation analysis for variable viscous couple stress fluid flow through a channel with non-uniform wall temperature. *Alex Eng J* 2016;55:69–75. <https://doi.org/10.1016/j.aej.2016.01.011>
 43. Ahmad B., Hayat T., Abbasi F. Hydromagnetic peristaltic transport of variable viscosity fluid with heat transfer and porous medium. *J Appl Math Inf Sci* 2016;10(6):2173–2181. <https://doi.org/10.18576/amis/100619>
 44. Tripathi B., Sharma B.K. Effect of variable viscosity on MHD inclined arterial blood flow with chemical reaction. *Int J Appl Mech Eng* 2018;23(3):767–785. <https://doi.org/10.2478/ijame-2018-0042>
 45. Mondal S.K., Pal D. Computational analysis of bio-convective flow of nanofluid containing gyrotactic microorganisms over a nonlinear stretching sheet with variable viscosity using HAM. *J Comput Des Eng* 2020;7(2):251–267. <https://doi.org/10.1093/jcde/qwaa021>
 46. Khan A., Farooq M., Nawaz R., Ayza H., Abu-Zinadah H. Analysis of couple stress fluid flow with variable viscosity using two homotopy-based methods. *Open Phys* 2021;19:134–145. <https://doi.org/10.1515/phys-2021-0015>
 47. Anwar T., Kumam P. A fractal fractional model for thermal analysis of GO–NaAlg–Gr hybrid nanofluid flow in a channel considering shape effects. *Case Stud Ther Eng* 2022;31:101828. <https://doi.org/10.1016/j.csite.2022.101828>
 48. Adnan F.A., Abdulhadi A.M. Effect of an inclined magnetic field on peristaltic flow of Bingham plastic fluid in an inclined symmetric channel with slip conditions. *Iraqi J Sci* 2019;60(7):1551–1574. <https://doi.org/10.24996/ijcs.2019.60.7.16>
 49. Vaidya H., Rajashekhar C., Manjunatha G., Prasad K.V., Makinde O.D., Vajravelu K. Influence of transport properties on the peristaltic MHD Jeffrey fluid flow through a porous asymmetric tapered channel. *Results Phys* 2020;18:103295. <https://doi.org/10.1016/j.rinp.2020.103295>
 50. Abbas Z., Rafiq M.Y. Analysis of heat and mass transfer phenomena in peristaltic transportation of hyperbolic tangent fluid in tapered channel. *Asia-Pac J Chem Eng* 2021;16(5):e2675. <https://doi.org/10.1002/apj.2675>
 51. Rafiq M.Y., Abbas Z., Ullah M.Z. Peristaltic mechanism of couple stress nanomaterial in a tapered channel. *Ain Shams Eng J* 2022;13(6):101779. <https://doi.org/10.1016/j.asej.2022.101779>
 52. Akram S., Athar M., Saeed K., Umair M.Y. Mechanism of double diffusive convection due to magnetized Williamson nanofluid flow in tapered asymmetric channel under the influence of peristaltic propulsion and radiative heat transfer. *Int J Numer Methods Heat Fluid Flow* 2023. <https://doi.org/10.1108/HFF-04-2023-0169>.